

Navigation Functions with non-Point Destinations and Moving Obstacles

Chuchu Chen, Caili Li and Herbert G. Tanner

Abstract—This paper formally expands the application domain of robot motion planning methods that are based on navigation functions to the case of moving obstacles. It generalizes the navigation function methodology from *static* sphere world environments, to *dynamic* ones. Specifically, it allows the obstacles’ locations to be time-varying, albeit unknown, and accommodates the case where the navigation goal is not a single isolated point, but rather a spherical manifold. For such cases, the paper presents analytical bounds on the tuning parameters that guarantee the navigation function properties of the time-varying potential function, uniformly in time. Thus using *the same* choice of tuning parameters, the agent is ensured that at every instance in time, the artificial potential field that directs it to its destination is free of local minima. The parameter bounds naturally depend on the geometry of the agent workspace, and include conditions on how close the obstacles can approach each other, the fixed workspace boundary, and the destination sphere. The bounds presented here are conservative; their analytic determination serves mainly the purpose of theoretically guaranteeing completeness properties for the methodology in the time-varying obstacle case.

I. INTRODUCTION AND RELATED WORK

Motion planning and obstacle avoidance strategies have been well established [1] in static and known environments, and have found application in a wide range of domains, from traditional areas like mobile robots [2] and manipulators [3], all the way to emerging ones such as self-driving vehicles [4]. Dynamic environments, however, present new challenges to motion planning and navigation [5]. Current application examples where a degree of automation is needed in dynamic environments include connected and automated vehicles [6], unmanned aerial vehicle (UAV) formations [7], and human-robot interaction [8], [9].

Among the challenges of motion planning and navigation in dynamic environments, is that *path planning* and *trajectory generation* are temporarily coupled and have to be solved concurrently in real-time [5]. Because different instantiations of the problem are being solved over time, it is not always clear how to establish global completeness and convergence guarantees. In existing literature, approaches to the problem of motion planning in dynamic environments fall roughly into two categories, distinguished based on whether path planning and trajectory generation are solved in (rapid) succession or concurrently.

Examples in the former category include approaches involving some kind of search-based method [10], [11] (e.g. A^* or D^*), and sampling methods [12] such as randomly

exploring random tree (RRT) [13], [14] or probabilistic roadmap method (PRM) [15], [16]. Search and sampling methods require spatial discretization and thus result in computation cost that increases markedly with the dimension of the workspace, and despite spectacular recent advances in processing speed, it is always a concern in high-dimensional problem instances. The challenge of a dynamic environment is treated in a variety of ways in the context of these methods, mainly either by fast re-generation of the roadmap or tree [16]–[18], or by treating time as another state variable [19], in the case where obstacle motion is predictable. In any case, search and sampling-based methods typically require a post-processing stage where the outcome of the planner needs to be “adapted” and morphed into a dynamically compatible reference trajectory for the actual vehicle to follow [20]; depending on the vehicle dynamics at hand, this is not always nontrivial and may require specific dynamic constraints on derivatives [21].

On the other end of the spectrum, namely with reference to methods that integrate path planning with trajectory generation, the dominant approach is arguably based on gradient descent methods. Parenthetically here, an interesting alternative to potential (or harmonic) fields is the velocity obstacle approach [22]–[25], which is conceptually related to artificial vector fields in the sense that it directly designates desired velocity vectors for the agent, but its reference velocities are not generated by a vector field; rather, they are produced in the form of admissible (velocity) sets, computed reactively over a through a short time horizon reachability computation that takes into account the agent’s dynamics. Naturally, the efficacy of velocity obstacle methods rests on the ability to accurately measure moving obstacle velocities at a reasonably high rate.

In the realm of potential field methods, and specifically in the context of applications of these techniques to dynamic environments, one still finds variations of the traditional potential field method that involves superposition of attractive and repulsive vector fields [26], [27], with the well-known limitations stemming from the appearance of local minima. Harmonic fields [28], which avoid the problem of local minima by integrating (numerically) Laplace’s equation, face challenges because of they would essentially require an iterative solution (in real time) of a nontrivial partial differential equation (PDE). The results here are limited, covering for instance cases of known (and constant) obstacle velocities [29], [30], or moving goal along a known trajectory [31].

While navigation functions [32], [33] can also ensure the absence of local minima, in the dynamic environment regime there has only been anecdotal evidence of their

This work was partially supported by DTRA under HDTRA1-16-1-0039. Chen and Tanner are with the Department of Mechanical Engineering, University of Delaware, Newark, DE 19716, USA. Email: {cchu, btanner}@udel.edu

efficacy (e.g. [34], [35]), and the various formal attempts to generalize this methodology to this regime [9], [36], [37] still leave some aspects uncovered [38]. Specifically, existing treatment of moving obstacles in the context of navigation functions [36] requires knowledge of obstacle motion and resorts to discontinuous (switching) control laws; comprehensive treatment of navigation function properties has been carried out for the case of a moving destination only [9], [37].

This paper addresses the problem of constructing navigation functions on sphere-worlds with moving obstacles. It contributes by offering analytic conditions on the geometric parameters of the time-varying workspace, under which the navigation function properties can be guaranteed *uniformly over time* for the same values of the navigation function tuning parameters. Only sketches of the mathematical proofs are provided here due to space limitations.

The rest of the paper will be organized as follows: First, the robot navigation problem and related terminology is introduced in Section II. Section III contains the main contribution of this paper: the theoretical analysis for the establishment of fixed bounds for the potential function tuning parameters, above which the potential function is guaranteed to be a navigation function uniformly over time. Section IV concludes and outlines directions for future work.

II. FORMAL PROBLEM STATEMENT

The workspace on which the navigation function is constructed is a sphere-world [33]. To avoid a detailed symbolic definition and listing of all geometric constructions describing the elements of this workspace, given the space restrictions this paper needs to adhere to, we provide an intuitive visual description of these constructs in Fig. 1.

The region within the mobile agent's state, x , is constrained to evolve is the interior of the ball of radius ρ_0 denoted $\mathcal{B}_0(\rho_0) \triangleq \{x \in \mathbb{R}^n \mid \beta_0 \triangleq \|x - o_0\|^2 - \rho_0^2 \leq 0\}$; for simplicity, hereafter the center of this ball is taken to be the origin: $o_0 = 0$. Interior obstacles are also assumed spherical, but the location of their centers is allowed to be time-varying. That is, obstacle $j \in \{1, \dots, m\} \subset \mathbb{N}$ has fixed radius ρ_j and a center that is denoted $o_j(t)$. The volume that obstacle j occupies is the interior of the ball $\mathcal{B}_j(t, \rho_j) \triangleq \mathcal{B}_j \triangleq \{x \in \mathbb{R}^n \mid \beta_j \triangleq \|x - o_j(t)\|^2 - \rho_j^2 \leq 0\}$. If the interior of \mathcal{B}_0 is "punctured" by all obstacles, the resulting set is *free workspace* denoted $\mathcal{F} \triangleq \mathcal{B}_0(\rho_0) \setminus \bigcup_{j=1}^m \mathcal{B}_j(t, \rho_j)$ (Fig. 1). A metric of the distance between the agent and the free space boundary is given by the product

$$\beta(x, t) = \prod_{j=0}^m \beta_j(x, o_j(t)) ,$$

where the dependence on obstacle motion is made explicit by presenting the obstacle center locations, $o_j(t)$, as a function of time.

Departing slightly from the majority of navigation function constructions, the one presented in this paper utilizes a non-point destination. This is because sometimes it is desirable for the agent to converge to a physical object or other agent, but stay at a certain small (safety) distance from it, rather than converge right onto it. For this reason, the navigation

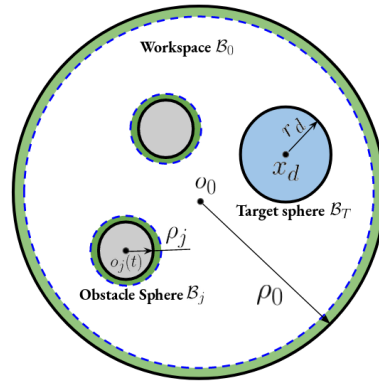


Fig. 1: An example of obstacles and target sphere in the agent's workspace: Blue and grey circles denote the target and obstacle spheres in the outer work space. Green rings mark neighborhoods of boundaries.

goal here is a spherical destination manifold, and any location on this manifold suffices as the final configuration for the agent. Naturally, the nondegeneracy condition for the navigation goal enforced by traditional formulations does not apply here; as it will be shown shortly, any point on the destination, or target, sphere is a degenerate critical point of the function. The target ball \mathcal{B}_T is assumed to be stationary at $x_d \in \mathcal{F}$ and have radius r_d . The boundary of the target ball is denoted $\partial\mathcal{B}_T = \{x \in \mathbb{R}^n \mid \|x - x_d\|^2 - r_d^2 = 0\}$ (Fig. 1). A metric of distance between the agent and the target sphere is coded by the goal function

$$J_i(x) = \left(\|x - x_d\|^2 - r_d^2 \right)^2 .$$

The agent's workspace is said to be *valid* if all objects, including obstacles, the target sphere, and the outer boundary are disjoint. This implies

$$\|o_j(t) - x_d\| > \rho_j + r_d, \quad \|x_d\| + r_d < \rho_0, \quad \|o_j\| + \rho_j < \rho_0 .$$

The goal of this paper is to prove the following statement:

Theorem 1. *Given a valid sphere-world \mathcal{F} , there exist an $N(\varepsilon) > 0$ such that for every fixed $k > N(\varepsilon)$ the function*

$$\varphi(x, t) = \frac{J(x)}{[J(x)^k + \beta(x, t)]^{1/k}} \quad (1)$$

is a navigation function on \mathcal{F} for a spherical target $\mathcal{B}_{x_d}(r_d)$, in the sense that all local minima of φ are on $\partial\mathcal{B}_{x_d}(r_d)$, and all other critical points of φ are non-degenerate.

III. APPROACH TO SOLUTION

A. Overview

Let $\mathcal{B}_j(\varepsilon) = \{x \in \mathbb{R}^n \mid 0 < \beta_j(x) < \varepsilon\}$ denote an ε -neighborhood of obstacle j (Fig. 1); in general, the notation $\mathcal{A}(\varepsilon)$ will be used to express an ε -neighborhood of the boundary of set \mathcal{A} . Let $\delta_d > 0$ be in the order of ε , and partition \mathcal{F} as follows.

- The set near obstacles and away from target: $\mathcal{F}_0(\varepsilon) \triangleq \bigcup_{j=1}^m \mathcal{B}_j(\varepsilon) \setminus \partial\mathcal{B}_T$
- the set near the (outer) workspace boundary: $\mathcal{F}_1(\varepsilon) \triangleq \mathcal{B}_0(\varepsilon) \setminus (\partial\mathcal{B}_T \cup \mathcal{F}_0(\varepsilon))$
- the set away from (any) workspace boundaries: $\mathcal{F}_2(\varepsilon) \triangleq \mathcal{F} \setminus (\partial\mathcal{B}_T \cup \partial\mathcal{F} \cup \mathcal{F}_0(\varepsilon) \cup \mathcal{F}_1(\varepsilon))$
- the set away from obstacles and target: $\mathcal{W}(\varepsilon) \triangleq \mathcal{F}_2(\varepsilon) \setminus \mathcal{B}_T(\delta_d)$.

The roadmap for establishing Theorem 1 is the following:

- 1) Verify that the target sphere is degenerate;
- 2) show that all critical points are in the interior of the \mathcal{F} ;
- 3) show that there are no critical points in $\mathcal{W}(\varepsilon)$ with appropriate tuning;
- 4) show that if \mathcal{F} is valid, there exist the upper bound on ε below which no local minima for φ can exist in $\mathcal{F}_0(\varepsilon)$;
- 5) show that if \mathcal{F} is valid, there is an upper bound on ε above which no critical point can exist in $\mathcal{F}_1(\varepsilon)$;
- 6) show that for an appropriately large k , any critical points in the interior of $\mathcal{F}_0(\varepsilon)$ are non-degenerate; and finally
- 7) show that any critical point within the target sphere is the local maximum.

B. Roadmap refinement

The technical analysis of this section utilizes a number of geometric constraints stemming mostly from workspace validity, and which are grouped listed in Table I.

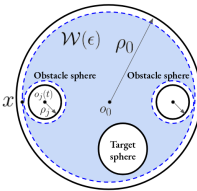
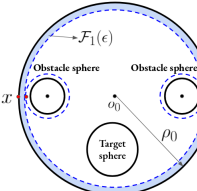
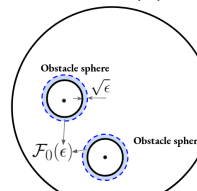
Cases	Constraints
$x \in \mathcal{W}(\varepsilon)$ 	$0 \leq \ x - o_0\ \leq \rho_0 - \sqrt{\varepsilon}$ $0 \leq \ o_0 - o_j\ \leq \rho_0 - \rho_j - \sqrt{\varepsilon}$ $0 < \ x - x_d\ < 2(\rho_0 - \sqrt{\varepsilon} - r_d)$ $r_d < \ x - o_j\ \leq 2\rho_0 - r_d$ $r_d + \rho_j < \ o_j - x_d\ < 2\rho_0 - 2\sqrt{\varepsilon}$
$x \in \mathcal{F}_1(\varepsilon)$ 	$\rho_0 - \varepsilon < \ x - o_0\ \leq \rho_0$ $0 \leq \ o_0 - o_j\ \leq \rho_0 - \rho_j - 2\sqrt{\varepsilon}$ $r_d < \ x - x_d\ < 2(\rho_0 - r_d)$ $\sqrt{\varepsilon + \rho_j^2} \leq \ x - o_j\ $ $\leq 2\rho_0 - \rho_j - 2\sqrt{\varepsilon}$ $r_d + \rho_j < \ o_j - x_d\ < 2\rho_0 - 2\sqrt{\varepsilon}$
$x \in \mathcal{F}_0(\varepsilon)$ 	$0 \leq \ x - o_0\ \leq \rho_0$ $0 \leq \ o_0 - o_j\ \leq \rho_0$ $r_d \leq \ x - x_d\ \leq 2\rho_0 - r_d$ $\rho_j \leq \ x - o_j\ \leq \rho_j + \sqrt{\varepsilon}$ $r_d + \rho_j + \sqrt{\varepsilon} < \ o_j - x_d\ $ $< 2\rho_0 - r_d - \sqrt{\varepsilon} - \rho_j$

TABLE I: Summary of constraints ensuring a valid workspace

Proposition 1. *If the workspace is valid, every $x_D \in \partial\mathcal{B}_T$, is a degenerate local minimum of φ . A vector v satisfying $v^\top \nabla^2 \varphi|_{x_D} v = 0$ is tangent to $\partial\mathcal{B}_T$.*

Proof. (Sketch) Take $x_D \in \partial\mathcal{B}_T$: $J|_{x_D} = 0$ and $\nabla|_{x_D} J = 0$. Evaluate

$$\nabla \varphi = \frac{1}{(J^k + \beta)^{2/k}} \left[(J^k + \beta)^{1/k} \nabla J - J \nabla (J^k + \beta)^{1/k} \right] \Big|_{x_D} \quad (2)$$

at x_D to verify that $\nabla \varphi|_{x_D} = 0$. To show that x_D is degenerate, pick a vector $v \in \mathbb{R}^n$, expand the quadratic form $v^\top \nabla^2 \varphi|_{x_D} v$ to see that

$$v^\top \nabla^2 \varphi|_{x_D} v = 8\beta^{-1/k} \|v^\top (x_D - x_d)\|^2 \geq 0 \quad (3)$$

with equality holding when $v^\top (x_D - x_d) = 0$.

Verify that v is normal to $(x_D - x_d)$, the radius direction of the target sphere, by evaluating their inner product. \square

Proposition 2. *If the workspace is valid, all critical points of φ are in the interior of \mathcal{F} .*

Proof. (Sketch) It suffices to show that no critical points exist in $\partial\mathcal{F}$. Take $x_0 \in \partial\mathcal{F}$; there exists an $l \in \{0, \dots, m\} \subset \mathbb{N}$ such that $x_0 \in \partial\mathcal{B}_l$. Hence, $\beta_l(x_0) = 0$ and $\nabla \beta_l|_{x_0} = 2(x_0 - o_l) \neq 0$. In a *valid workspace*, all obstacles are disjoint; therefore, $\forall j \in \{0, \dots, m\} \setminus \{l\}$, it is $\beta_j(x_0) > 0$. Then (2) evaluated at x_0 reduces to

$$\nabla \varphi|_{x_0} = -\frac{J^{-k}}{k} \prod_{j=0, j \neq l}^m \beta_j(x_0) \nabla \beta_l(x_0) \neq 0. \quad (4)$$

\square

Let us note at this point that it is known that φ and $\hat{\varphi} \triangleq \frac{J^k}{\beta}$ share the same critical points [32]. Thus much of the analysis is performed on $\hat{\varphi}$ for analytical expedience.

Proposition 3. *For every $\varepsilon > 0$ there exists an $N(\varepsilon) > 0$ such that if $k \geq N(\varepsilon)$ there are no critical points of $\hat{\varphi} = \frac{J^k}{\beta}$ in $\mathcal{W}(\varepsilon)$.*

Proof. (Sketch) At any critical point, $\beta \nabla J - \frac{1}{k} \nabla \beta = 0$, meaning $k = \frac{J \|\nabla \beta\|}{\beta \|\nabla J\|}$. Thus, if $k > \frac{J \|\nabla \beta\|}{\beta \|\nabla J\|}$ there can be no critical points in $\mathcal{W}(\varepsilon)$. It suffices to have

$$k \geq \sup_{\mathcal{W}} \frac{J}{\|\nabla J\|} \sup_{\mathcal{W}} \frac{\|\nabla \beta\|}{\beta} > \frac{J \|\nabla \beta\|}{\beta \|\nabla J\|}.$$

Let β_j be the obstacle closest to the critical point. Note that when $x \in \mathcal{W}(\varepsilon)$, $\beta_j \geq \varepsilon$, and from Table I bounds for $\sup_{\mathcal{W}} \frac{J}{\|\nabla J\|}$ and $\sup_{\mathcal{W}} \frac{\|\nabla \beta\|}{\beta}$ are established in $\mathcal{W}(\varepsilon)$:

$$\sup_{\mathcal{W}} \frac{J}{\|\nabla J\|} = \sup_{\mathcal{W}} \frac{\|x - x_d\|^2 - r_d^2}{4\|x - x_d\|} = \frac{1}{2}(\rho_0 - \sqrt{\varepsilon})$$

$$\sup_{\mathcal{W}} \frac{\|\nabla \beta\|}{\beta} \leq \frac{2}{\varepsilon} \left[(2m+1)(\rho_0 - \sqrt{\varepsilon}) - m\rho_j \right].$$

To avoid critical points, it suffices to have $k \geq N(\varepsilon)$ where

$$N(\varepsilon) \triangleq \frac{1}{\varepsilon^2} (\rho_0 - \sqrt{\varepsilon})^2 \left[1 + 2m + \frac{m\rho_j}{\rho_0 - \sqrt{\varepsilon}} \right]. \quad (5)$$

\square

Proposition 4. *In any valid workspace, $\exists \varepsilon_0$ such that $\hat{\varphi} = \frac{J^k}{\beta}$ has no local minima in $\mathcal{F}_0(\varepsilon)$, as long as $\varepsilon < \varepsilon_0$.*

Proof. (Sketch) A critical point of $\hat{\varphi}$ is not a local minimum if the Hessian of $\hat{\varphi}$ has at least one negative eigenvalue there. Essentially, it amounts to showing that $v^\top \nabla^2 \hat{\varphi} v < 0$ for some vector $v \in \mathbb{R}^n$. Take $x_c \in \mathcal{F}_0(\varepsilon)$ to be that critical point of $\hat{\varphi}$. From Table I and for $x_c \in \mathcal{F}_0(\varepsilon)$

$$0 < \|x - o_j(t)\| - \rho_j < \sqrt{\varepsilon} < \|o_j(t) - x_d\| - r_d - \rho_j. \quad (6)$$

Function β can always be factored as $\beta = \beta_q \prod_{p \in \{0, \dots, m\} \setminus \{q\}} \beta_p$ where $\bar{\beta}_q \triangleq \prod_{p \in \{0, \dots, m\} \setminus \{q\}} \beta_p$ is referred to as the *omitted product* [32]. Vector $\nabla \beta$ expands

$$\begin{aligned} \nabla \beta &= \sum_{l=1}^m 2(x_c - o_l(t)) \bar{\beta}_l - 2\bar{\beta}_0 x_c \\ &= 2(x_c - o_j(t)) \bar{\beta}_j + \beta_j \underbrace{\left[2 \sum_{l=1, l \neq j}^m (x_c - o_l(t)) \frac{\bar{\beta}_l}{\beta_j} - 2 \frac{\bar{\beta}_0}{\beta_j} x_c \right]}_{\alpha_j} \\ &= 2(x_c - o_j(t)) \bar{\beta}_j + \beta_j \alpha_j. \quad (7) \end{aligned}$$

Selecting $k \geq N(\varepsilon)$ based on (5), and defining

$$C_k \triangleq \frac{1}{\varepsilon} (\rho_0 - \sqrt{\varepsilon})^2 \left(1 + 2m + \frac{m\rho_j}{\rho_0 - \sqrt{\varepsilon}} \right) \quad (8)$$

to shorten the analytical expressions, one can choose $k := \frac{C_k}{\varepsilon}$.

For x_c not to be a local minimum, it suffices to show that for some vector v and small enough ε , $v^\top \nabla^2 \phi(x_c) v < 0$.

Take \hat{v} orthogonal to $\frac{\nabla \beta_j}{\|\nabla \beta_j\|}$. Then

$$\begin{aligned} \frac{\beta^2}{J^{k-1}} \hat{v}^\top \nabla^2 \phi|_{x_c} \hat{v} &= 2J \underbrace{\left[\frac{(x_c - o_j(t))^\top (x_c - x_d)}{\|x_c - x_d\|^2} - 1 \right]}_{\text{Part A}} \\ &\quad + \frac{(\varepsilon \sqrt{J} |\hat{v}^\top \alpha_j|)^2 \sqrt{J} (x_c - o_j(t))^\top (x_c - x_d)}{4(C_k \bar{\beta}_j)^2 \|x_c - x_d\|^2} \\ &+ \beta_j \left[\frac{\hat{v}^\top \nabla^2 J \hat{v}}{16 \|x_c - x_d\|^2} \nabla \bar{\beta}_j^\top \nabla J + J \hat{v}^\top \left(\frac{1 - \frac{1}{k}}{\bar{\beta}_j} \nabla \bar{\beta}_j \nabla \bar{\beta}_j^\top - \nabla^2 \bar{\beta}_j \right) \hat{v} \right]. \end{aligned}$$

For Part A we know [32, Lemma 3.5]

$$\begin{aligned} \frac{(x_d - o_j(t))^\top (x_c - x_d)}{\|x_c - x_d\|^2} - 1 &\leq \frac{\|x_d - o_j(t)\| \left(\sqrt{\varepsilon + \rho_j^2} - \|x_d - o_j(t)\| \right)}{\|x_c - x_d\|^2}. \end{aligned}$$

It follows that

$$\begin{aligned} \frac{\beta^2}{J^{k-1}} \hat{v}^\top \nabla^2 \phi|_{x_c} \hat{v} &\leq \frac{2J \|x_d - o_j(t)\| \left(\sqrt{\varepsilon + \rho_j^2} - \|x_d - o_j(t)\| \right)}{\|x_c - x_d\|^2} \\ &+ \varepsilon \frac{\hat{v}^\top \nabla^2 J \hat{v}}{16 \|x_c - x_d\|^2} \nabla \bar{\beta}_j^\top \nabla J J \hat{v}^\top \left(\frac{1 - \frac{1}{k}}{\bar{\beta}_j} \nabla \bar{\beta}_j \nabla \bar{\beta}_j^\top - \nabla^2 \bar{\beta}_j \right) \hat{v} \\ &+ \varepsilon \sup_{\mathcal{F}_0(\varepsilon)} \frac{(\sqrt{J\varepsilon} |\hat{v}^\top \alpha_j|)^2 \sqrt{J} [x_d - o_j(t)]^\top (x_c - x_d)}{4(C_k \bar{\beta}_j)^2 \|x_c - x_d\|^2}. \quad (9) \end{aligned}$$

The last two terms in the right hand side of (9) can be made arbitrary small by choosing ε appropriately small, and thus the first term will dominate. The sign of the latter is determined by $\sqrt{\varepsilon + \rho_j^2} - \|x_d - o_j(t)\|$ which (6) guarantees to be negative. \square

Proposition 5. For any valid workspace, there exist $k_1 > 0$ and $\varepsilon_1 > 0$ such that $\hat{\phi}$ has no critical points in $\mathcal{F}_1(\varepsilon)$, as long as $\varepsilon < \varepsilon_1$ and

$$k > k_1 \triangleq \frac{m}{\varepsilon} \left(\frac{\rho_0^2 - \rho_0 r_d}{2\rho_0 - r_d} \right) (2\rho_0 - \rho_j - 2\sqrt{\varepsilon}). \quad (10)$$

Proof. (Sketch) For nonexistence of critical points in $\mathcal{F}_1(\varepsilon)$, it suffices to show that $\nabla \hat{\phi}^\top \nabla J > 0$ there.

Take $x_c \in \mathcal{F}_1(\varepsilon)$ and expand

$$\nabla J^\top \nabla \beta_0 = 8 \underbrace{\left(\|x_c - x_d\|^2 - r_d^2 \right)}_{>0} \underbrace{\|x_c\|}_{>0} \underbrace{\left(\|x_d\| - \|x_c\| \right)}_{<0} < 0.$$

Evaluate

$$\begin{aligned} \nabla \hat{\phi}^\top \nabla J &= \left[\frac{kJ^{k-1}}{\beta^2} \left(\beta \nabla J - \frac{1}{k} J \nabla \beta \right) \right]^\top \nabla J \\ &> \frac{J^k \beta_0}{\beta^2} \left[16k \bar{\beta}_0 \|x_c - x_d\|^2 - \nabla \bar{\beta}_0^\top \nabla J \right]. \end{aligned}$$

To ensure $\nabla \hat{\phi}^\top \nabla J > 0$, select k as

$$\begin{aligned} k &> \frac{\nabla \bar{\beta}_0^\top \nabla J}{16 \bar{\beta}_0 \|x_c - x_d\|^2} \\ &> \frac{1}{\varepsilon} \sup_{\mathcal{F}_1} \left(\frac{\|x_c - x_d\|^2 - r_d^2}{2 \|x_c - x_d\|} \right) \sum_{l=1}^m \left(\sup_{\mathcal{F}_1} \left(\|x_c - o_l(t)\| \right) \right) \\ &\geq \frac{m}{\varepsilon} \left(\frac{\rho_0^2 - \rho_0 r_d}{2\rho_0 - r_d} \right) (2\rho_0 - \rho_j - 2\sqrt{\varepsilon}) = k_1. \end{aligned}$$

Now define

$$\varepsilon_a \triangleq \rho_0^2 - r_d^2 \quad \varepsilon_b \triangleq \frac{1}{4} (\rho_0 - \rho_j)^2 \quad \varepsilon_c \triangleq \frac{1}{9} (2\rho_0 - \rho_j)^2$$

and pick $\varepsilon < \min\{\varepsilon_a, \varepsilon_b, \varepsilon_c\}$ in conjunction with $k > k_1$ to guarantee no critical points in $\mathcal{F}_1(\varepsilon)$. \square

Proposition 6. With appropriate choice of k , critical points x_c in the interior of $\mathcal{F}_0(\varepsilon)$ are non-degenerate.

Proof. (Sketch) One way to establish non-degeneracy is to split the tangent space of $\hat{\phi}$ at the critical point into two partitions, and ensure that the quadratic form with matrix $\nabla^2 \hat{\phi}$ is positive on one partition and negative on the other [32, Lemma 3.8].

In the subspace that is orthogonal to $\frac{\nabla \beta_j}{\|\nabla \beta_j\|}$, the proof of Proposition 4 established that the quadratic form is negative at critical points $x_c \in \mathcal{F}_0(\varepsilon)$.

Take $v = \widehat{\nabla \beta_j} \triangleq \frac{\nabla \beta_j}{\|\nabla \beta_j\|}$. We will show that $v^\top \nabla^2 \phi v > 0$.

Indeed, to verify the sign of $\widehat{\nabla \beta_j}^\top \nabla^2 \hat{\phi} \widehat{\nabla \beta_j}$, expand

$$\begin{aligned} \frac{\beta^2}{J^{k-1}} \widehat{\nabla \beta_j}^\top \nabla^2 \hat{\phi} \widehat{\nabla \beta_j} &= \widehat{\nabla \beta_j}^\top k \beta \nabla^2 J \widehat{\nabla \beta_j} \\ &+ \frac{J}{\beta} \left(1 - \frac{1}{k} \right) \left(\nabla \beta^\top \widehat{\nabla \beta_j} \right)^2 - J \widehat{\nabla \beta_j}^\top \nabla^2 \beta \widehat{\nabla \beta_j} \quad (11) \end{aligned}$$

and note that for small enough ε [32]

$$\frac{J \|\nabla \beta\|^2}{2k\beta} + \frac{J}{\beta} \left(1 - \frac{1}{k} \right) \left(\nabla \beta^\top \widehat{\nabla \beta_j} \right)^2 - J \widehat{\nabla \beta_j}^\top \nabla^2 \beta \widehat{\nabla \beta_j} \geq 0.$$

Then to set the sign of (11), it suffices to make

$$\widehat{\nabla \beta_j}^\top k \beta \nabla^2 J \widehat{\nabla \beta_j} \geq \frac{J \|\nabla \beta\|^2}{2k\beta}. \quad (12)$$

Recall that critical points are assumed here to be in the interior of $\mathcal{F}_0(\varepsilon)$. Table I indicates that $\|x_c - x_d\| > r_d$. Assume x_c to be in the vicinity of \mathcal{B}_j , and allow r_d to be expressed as $r_d = \zeta \inf_{\mathcal{B}_j(\varepsilon)} \|x_c - x_d\|$ for an appropriate scalar $0 < \zeta < 1$. By expanding both sides of (12) and bounding terms on the way, one concludes that (12) is implied by

$$\left(\frac{(x_c - o_j(t))^T (x_c - x_d)}{\|x_c - o_j(t)\| \|x_c - x_d\|} \right)^2 \geq \frac{1 + \zeta^2}{2}. \quad (13)$$

An independent derivation establishes that

$$\frac{(x_c - o_j(t))^T (x_c - x_d)}{\|x_c - o_j(t)\| \|x_c - x_d\|} \geq 1 - \frac{\varepsilon \|\alpha_j\|}{\beta_j \|x_c - o_j(t)\|}. \quad (14)$$

Thus to satisfy (13) it suffices to choose ε sufficiently small so that

$$\begin{aligned} 1 - \frac{\varepsilon \|\alpha_j\|}{\beta_j \|x_c - o_j(t)\|} &> \sqrt{\frac{1 + \zeta^2}{2}} \\ \implies \varepsilon < \left(1 - \sqrt{\frac{1 + \zeta^2}{2}} \right) \frac{\rho_j^m}{2(m-1)(2\rho_0)^{2m-3}}. \end{aligned} \quad (15)$$

□

Proposition 7. *There exists $k_0 > 0$, such that $\forall k > k_0$, any critical point x_c in the interior of \mathcal{B}_T is a local maximum of $\hat{\phi} = \frac{J^k}{\beta}$.*

Proof. (Sketch) There are only two cases a critical point in the interior of \mathcal{B}_T : it is either the \mathcal{B}_T sphere center, or any other point in the interior.

1) *Case A:* Assume x_c is the center of \mathcal{B}_T , and let us denote the latter x_d . Then $\nabla J|_{x_d} = 0$. To show that x_c is a local maximum, it suffices to show $\nabla^2 \left(\frac{J^k}{\beta} \right)|_{x_d}$ is negative definite. Pick any unit vector $q \in \mathbb{R}^n$ and compute

$$\frac{\beta^2}{J^{k-2}} q^T \nabla^2 \left(\frac{J^k}{\beta} \right)|_{x_d} q = -4k^2 \beta r_d^6 - k r_d^8 q^T \nabla^2 \beta q.$$

To make this expression negative one picks:

$$k > k_2 \triangleq \frac{m}{4} r_d^{2-2m} \|2\rho_0 - \rho_j - r_d\|^{2m-4}. \quad (16)$$

2) *Case B:* Take $x_c \in \mathcal{B}_T \setminus (\partial \mathcal{B}_T \cup \{x_d\})$. Any unit vector $q \in \mathbb{R}^n$, can be expressed as a linear combination of two unit orthogonal vectors $v_1 = \frac{\nabla J}{\|\nabla J\|}$ and vector $v_2 \perp v_1$.

Now note that

$$\begin{aligned} \frac{\beta^2}{J^{k-2}} q^T \nabla^2 \left(\frac{J^k}{\beta} \right)|_{x_c} q &\leq -4k\beta J^{3/2} \\ &+ J^2 \left(\frac{\|\nabla \beta\|^2}{\beta} + |v_1^T \nabla^2 \beta v_1| + |v_1^T \nabla^2 \beta v_2| + |v_2^T \nabla^2 \beta v_2| \right). \end{aligned}$$

Therefore, the quadratic form becomes negative if

$$\begin{aligned} k > k_3 \triangleq \frac{r_d^2}{4(r_d - \delta_d)^{2m}} \left[\frac{m \left(\|2\rho_0 - \rho_j\|^2 - \rho_j^2 \right)^{2m-2}}{(r_d - \delta_d)^{2m}} \right. \\ \left. + 3m(m-1) \left(\|2\rho_0 - \rho_j\|^2 - \rho_j^2 \right)^{m-2} \right]. \end{aligned}$$

Thus selecting $k > k_0 = \max\{k_2, k_3\}$ guarantees that any critical point in the interior of \mathcal{B}_T is a local maximum. □

C. Summary

We can summarize the bounds derived within each proof for the tuning parameter k and the proximity to workspace boundary parameter ε , in Tables II and III, respectively.

Propositions	Lower bounds on k
Props. 3 & 4	$k \geq \frac{1}{\varepsilon^2} (\rho_0 - \sqrt{\varepsilon}) \left[1 + 2m + \frac{m\rho_j}{\rho_0 - \sqrt{\varepsilon}} \right]$
Prop. 5	$k \geq \frac{m}{\varepsilon} \left(\frac{\rho_0^2 - \rho_0 r_d}{2\rho_0 - r_d} \right) (2\rho_0 - \rho_j - 2\sqrt{\varepsilon})$
Prop. 7	$k > \frac{m}{4} r_d^{2-2m} \ 2\rho_0 - \rho_j - r_d\ ^{2m-4}$ $k > \frac{r_d^2}{4(r_d - \delta_d)^{2m}} \left[\frac{m \left(\ 2\rho_0 - \rho_j\ ^2 - \rho_j^2 \right)^{2m-2}}{(r_d - \delta_d)^{2m}} + 3m(m-1) \left(\ 2\rho_0 - \rho_j\ ^2 - \rho_j^2 \right)^{m-2} \right]$

TABLE II: Summary of bounds on k in different propositions. An admissible value for k satisfies the conjunction of the above conditions.

Propositions	Upper bounds on ε
Prop. 3	$0 < \varepsilon$
Prop. 4	$0 < \varepsilon < (r_d + \rho_j)^2 - \rho_j^2$
Prop. 5	$0 < \varepsilon < \rho_0^2 - r_d^2$ $0 < \varepsilon < \frac{1}{4} (\rho_0 - \rho_j)^2$ $0 < \varepsilon < \frac{1}{9} (2\rho_0 - \rho_j)^2$
Prop. 6	$0 < \varepsilon < \left(1 - \sqrt{\frac{1 + \zeta^2}{2}} \right) \frac{\rho_j^m}{2(m-1)(2\rho_0)^{2m-3}}$

TABLE III: Summary of bounds on ε in different propositions. An admissible value for ε satisfies the conjunction of the above conditions.

IV. CONCLUSIONS AND FUTURE WORK

Navigation functions can be constructed for problem instances with moving obstacles. There exist choices of the tuning parameter for the function that guarantee the properties of the navigation function, uniformly in time, as long as certain geometric conditions related to the validity of the workspace are ensured. The paper provides explicit expressions for bounds, above which the tuning parameter is guaranteed to yield a navigation function for all time; however one should keep in mind that these bounds have been derived considering the worst possible cases, and can therefore be very conservative. Typically, effective tuning can be achieved at much lower values; nonetheless, the establishment of those bounds theoretically guarantees the persistence of navigation function properties over time, for the same fixed parameter values. Several interesting extensions of this work can be imagined, including star-shaped obstacles (cf. [9]) and multi-agent settings (cf. [39]).

REFERENCES

- [1] J. Minguez, F. Lamiroux, and J. P. Laumond, *Motion planning and obstacle avoidance*. Springer, 2016.
- [2] A. Pandey, S. Pandey, and D. R. Parhi, "Mobile robot navigation and obstacle avoidance techniques: A review," *International Robotics & Automation Journal*, vol. 2, no. 3, pp. 96–105, 2017.
- [3] H. Tanner and K. Kyriakopoulos, "Nonholonomic motion planning for mobile manipulators," *Transactions on Robotics and Automation*, pp. 1233–1238, 2000.
- [4] D. González, J. Pérez, V. Milanés, and F. Nashashibi, "A review of motion planning techniques for automated vehicles," *Transactions on Intelligent Transportation Systems*, vol. 17, no. 4, pp. 1135–1145, 2015.
- [5] M. Mohanan and A. Salgoankar, "A survey of robotic motion planning in dynamic environments," *Robotics and Autonomous Systems*, vol. 100, pp. 171–185, 2018.
- [6] L. Fernandes, J. Souza, P. Shinzato, G. Pessin, C. C. Mendes, F. S. Osório, and D. F. Wolf, "Intelligent robotic car for autonomous navigation: Platform and system architecture," in *Proceedings of the IEEE Second Brazilian Conference on Critical Embedded Systems*, 2012, pp. 12–17.
- [7] P. Yao, H. Wang, and Z. Su, "Real-time path planning of unmanned aerial vehicle for target tracking and obstacle avoidance in complex dynamic environment," *Aerospace Science and Technology*, vol. 47, pp. 269–279, 2015.
- [8] E. Prassler, J. Scholz, and P. Fiorini, "A robotics wheelchair for crowded public environment," *IEEE Robotics & Automation Magazine*, vol. 8, no. 1, pp. 38–45, 2001.
- [9] C. Li and H. Tanner, "Navigation functions with time-varying destination manifolds in star worlds," *Transactions on Robotics*, vol. 35, no. 1, pp. 35–48, 2018.
- [10] Z. Ajanovic, B. Lacevic, B. Shyrokau, M. Stolz, and M. Horn, "Search-based optimal motion planning for automated driving," in *Proceedings of the IEEE/RSJ International Conference on Intelligent Robots and Systems*, 2018, pp. 4523–4530.
- [11] D. Ferguson and A. Stentz, "Using interpolation to improve path planning: The field D* algorithm," *Journal of Field Robotics*, vol. 23, no. 2, pp. 79–101, 2006.
- [12] M. Elbanhawi and M. Simic, "Sampling-based robot motion planning: A review," *Access*, vol. 2, pp. 56–77, 2014.
- [13] M. Zucker, J. Kuffner, and M. Branicky, "Multipartite RRTs for rapid replanning in dynamic environments," in *Proceedings of the IEEE International Conference on Robotics and Automation*, 2007, pp. 1603–1609.
- [14] C. Fulgenzi, A. Spalanzani, and C. Laugier, "Probabilistic rapidly-exploring random trees for autonomous navigation among moving obstacles," in *Proceedings of the IEEE International Conference on Robotics and Automation*, 2009, pp. 4027–4033.
- [15] J. P. Van Den Berg, D. Nieuwenhuisen, L. Jaillet, and M. Overmars, "Creating robust roadmaps for motion planning in changing environments," in *Proceedings of the IEEE/RSJ International Conference on Intelligent Robots and Systems*, 2005, pp. 1053–1059.
- [16] L. Jaillet and T. Siméon, "A PRM-based motion planner for dynamically changing environments," in *Proceedings of the IEEE/RSJ International Conference on Intelligent Robots and Systems*, vol. 2, 2004, pp. 1606–1611.
- [17] J. P. Van Den Berg and M. H. Overmars, "Roadmap-based motion planning in dynamic environments," *Transactions on Robotics*, vol. 21, no. 5, pp. 885–897, 2005.
- [18] J. Van Den Berg and M. Overmars, "Kinodynamic motion planning on roadmaps in dynamic environments," in *Proceedings of the IEEE/RSJ International Conference on Intelligent Robots and Systems*, 2007, pp. 4253–4258.
- [19] J. Van den Berg and M. Overmars, "Path planning in repetitive environments," in *Proceedings of the International Conference on Methods and Models in Automation and Robotics*, 2006, pp. 657–662.
- [20] S. Lindemann and S. LaValle, "Current issues in sampling-based motion planning," pp. 36–54, 2005.
- [21] D. Mellinger and V. Kumar, "Minimum snap trajectory generation and control for quadrotors," in *Proceedings of the IEEE International Conference on Robotics and Automation*, 2011, pp. 2520–2525.
- [22] P. Fiorini and Z. Shiller, "Motion planning in dynamic environments using velocity obstacles," *The International Journal of Robotics Research*, vol. 17, no. 7, pp. 760–772, 1998.
- [23] F. L., C. Laugier, and Z. Shiller, "Navigation among moving obstacles using the NLVO: Principles and applications to intelligent vehicles," *Autonomous Robots*, vol. 19, no. 2, pp. 159–171, 2005.
- [24] D. W., J. Van Den Berg, and D. M., "Generalized velocity obstacles," in *Proceedings of the IEEE/RSJ International Conference on Intelligent Robots and Systems*, 2009, pp. 5573–5578.
- [25] J. Van den Berg, M. Lin, and D. Manocha, "Reciprocal velocity obstacles for real-time multi-agent navigation," in *Proceedings of the IEEE International Conference on Robotics and Automation*, 2008, pp. 1928–1935.
- [26] V. Olunloyo and M. Ayomoh, "Autonomous mobile robot navigation using hybrid virtual force field concept," *European journal of scientific research*, vol. 31, no. 2, pp. 204–228, 2009.
- [27] O. Montiel, U. Orozco-Rosas, and R. Sepúlveda, "Path planning for mobile robots using bacterial potential field for avoiding static and dynamic obstacles," *Expert Systems with Applications*, vol. 42, no. 12, pp. 5177–5191, 2015.
- [28] C. Connolly, "Harmonic functions and collision probabilities," *The International Journal of Robotics Research*, vol. 16, no. 4, pp. 497–507, 1997.
- [29] S. Aiushita, T. Hisanobu, and S. Kawamura, "Fast path planning available for moving obstacle avoidance by use of laplace potential," in *Proceedings of the IEEE International Conference on Robotics and Automation*, 1993, pp. 673–678.
- [30] S. Waydo and R. Murray, "Vehicle motion planning using stream functions," in *Proceedings of the IEEE International Conference on Robots and Systems*, 2003, pp. 2484–2491.
- [31] P. Szulczyński, D. Pazderski, and K. Kozłowski, "Harmonic functions and collision probabilities," *Journal of Automation Mobile Robotics and Intelligent Systems*, vol. 5, no. 3, pp. 497–507, 2011.
- [32] D. E. Koditschek and E. Rimon, "Robot navigation functions on manifolds with boundary," *Advances in Applied Mathematics*, vol. 11, no. 4, pp. 412–442, 1990.
- [33] E. Rimon and D. Koditschek, "Exact robot navigation using artificial potential functions," *Transactions on Robotics and Automation*, vol. 8, no. 5, pp. 501–518, 1992.
- [34] S. Iizuka, T. Nakamura, and S. Suzuki, "Robot navigation in dynamic environment using navigation function APF with SLAM," in *Proceedings of the IEEE 8th Europe-Asia Congress on Mechatronics*, 2014, pp. 89–92.
- [35] N. Pradhan, T. Burg, and S. Birchfield, "Robot crowd navigation using predictive position fields in the potential function framework," in *Proceedings of American Control Conference*, 2011, pp. 4628–4633.
- [36] S. G. Loizou, H. G. Tanner, V. Kumar, and K. Kyriakopoulos, "Closed loop navigation for mobile robots in dynamic environments," in *Proceedings of The IEEE/RSJ International Conference on Robots and Systems*, 2003, pp. 3769–3774.
- [37] J. Sun and T. Herbert, G., "Constrained decision-making for low-count radiation detection by mobile sensors," *Autonomous Robots*, vol. 39, no. 4, pp. 519–536, 2015.
- [38] N. Shvalb and S. Hacoheh, "Motion in potential field and navigation function," *Autonomous Mobile Robots and Multi-Robot Systems: Motion-Planning, Communication, and Swarming*, pp. 87–107, 2019.
- [39] I. Yadav, K. Eckenhoff, G. Huang, and H. G. Tanner, "Visual-inertial target tracking and motion planning for UAV-based radiation detection," *arXiv preprint arXiv:1805.09061*, 2018.